UNIVERSIDADE DE COIMBRA

FACULDADE DE CIÊNCIAS E TECNOLOGIA

HEAT GENERATION WHEN FORMING AHSS: EXPERIMENTAL AND NUMERICAL ANALYSIS OF TENSILE AND DRAW-BEAD TESTS

D.M. Neto[1] • J.R. Barros[1] • M.C. Oliveira[1] • P.V. Antunes[1] • A. Ramalho[1] • R.L. Amaral[2] • A.D. Santos[2] • J.L. Alves[3] • L.F. Menezes[1]

[1] University of Coimbra, CEMMPRE, Department of Mechanical Engineering, Portugal

[2] University of Porto, Faculty of Engineering, Portugal

[2] University of Minho, CMEMS, Department of Mechanical Engineering, Portugal

IDDRG 2020

Virtual IDDRG 2020 conference

26th-30th October 2020

Korea

Advanced High Strength Steels (AHSS)

- Adopted in the **automotive industry**
  - ✓ High strength and also good formability
  - ✓ Lower thickness of the sheet steels
  - ✓ Reduce the overall weight of the vehicles
  - ✓ Reduce fuel consumption
  - ✓ Reduce emissions of greenhouse gases in the atmosphere

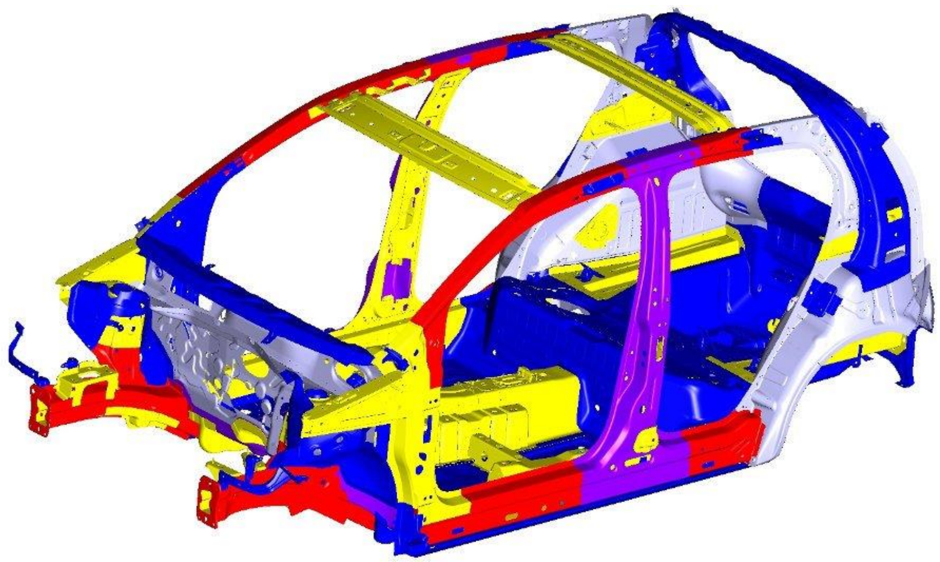

- **Limited wide application** in the automotive industry
  - ✓ Challenges in formability
  - ✓ Life of the forming tools
  - ✓ Springback behavior

Sheet metal forming process

- **Sheet metal forming** of AHSS
  - ✓ Large contact pressures on the tools
  - ✓ Large frictional forces on the tools
  - ✓ Parts susceptible to surface damage

- **Thermal analysis** of the sheet metal forming process
  - ✓ **Heat generated by plastic deformation**
  - ✓ **Heat generated by frictional contact sliding**
  - ✓ Heat losses to the environment
  - ✓ Heat losses to the forming tools

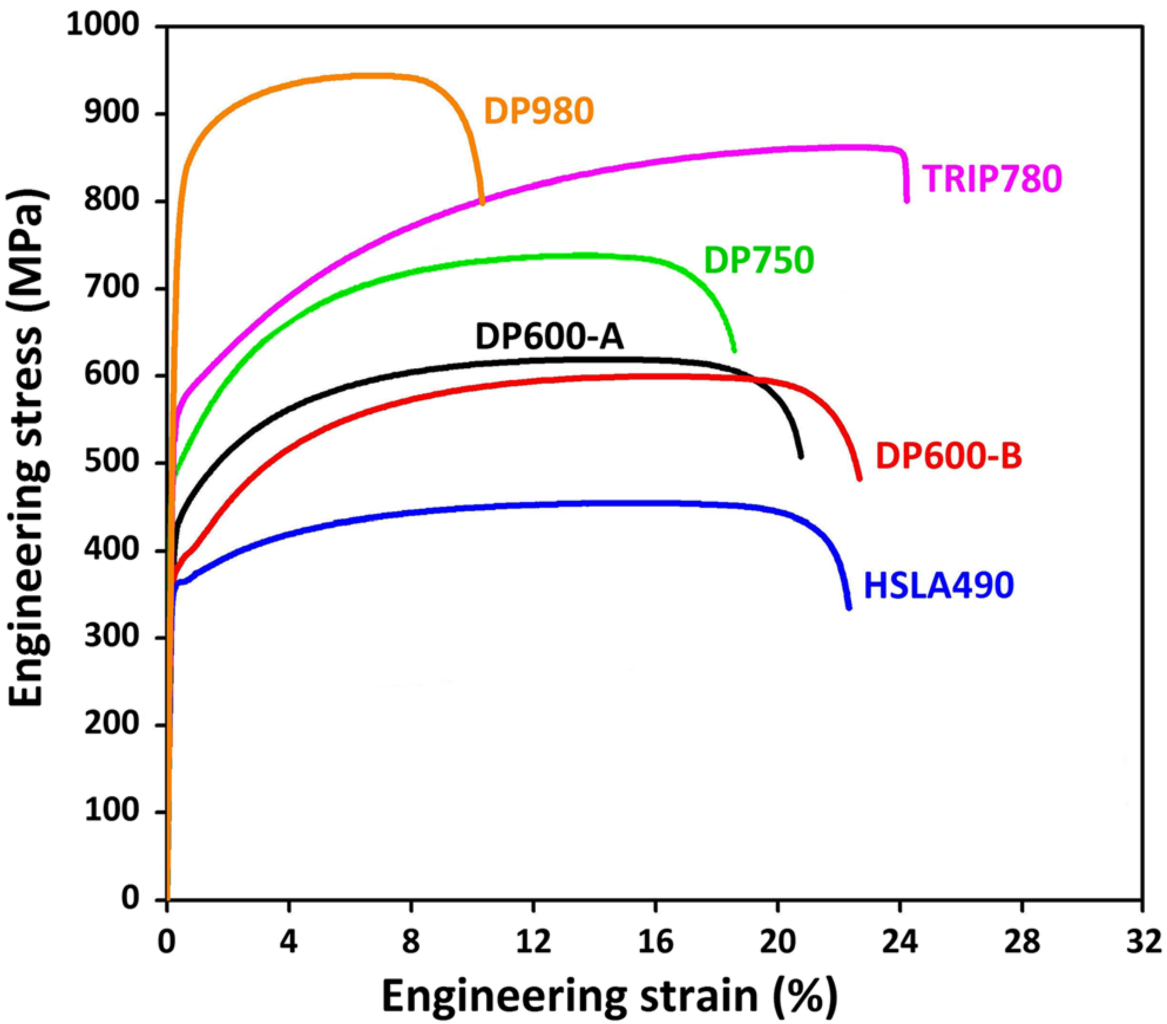

Frictional conditions at the interface

- Different **tribological tests** have been developed
  - ✓ Comprise typical forming operations
  - ✓ Reproduce the tribological conditions of forming processes

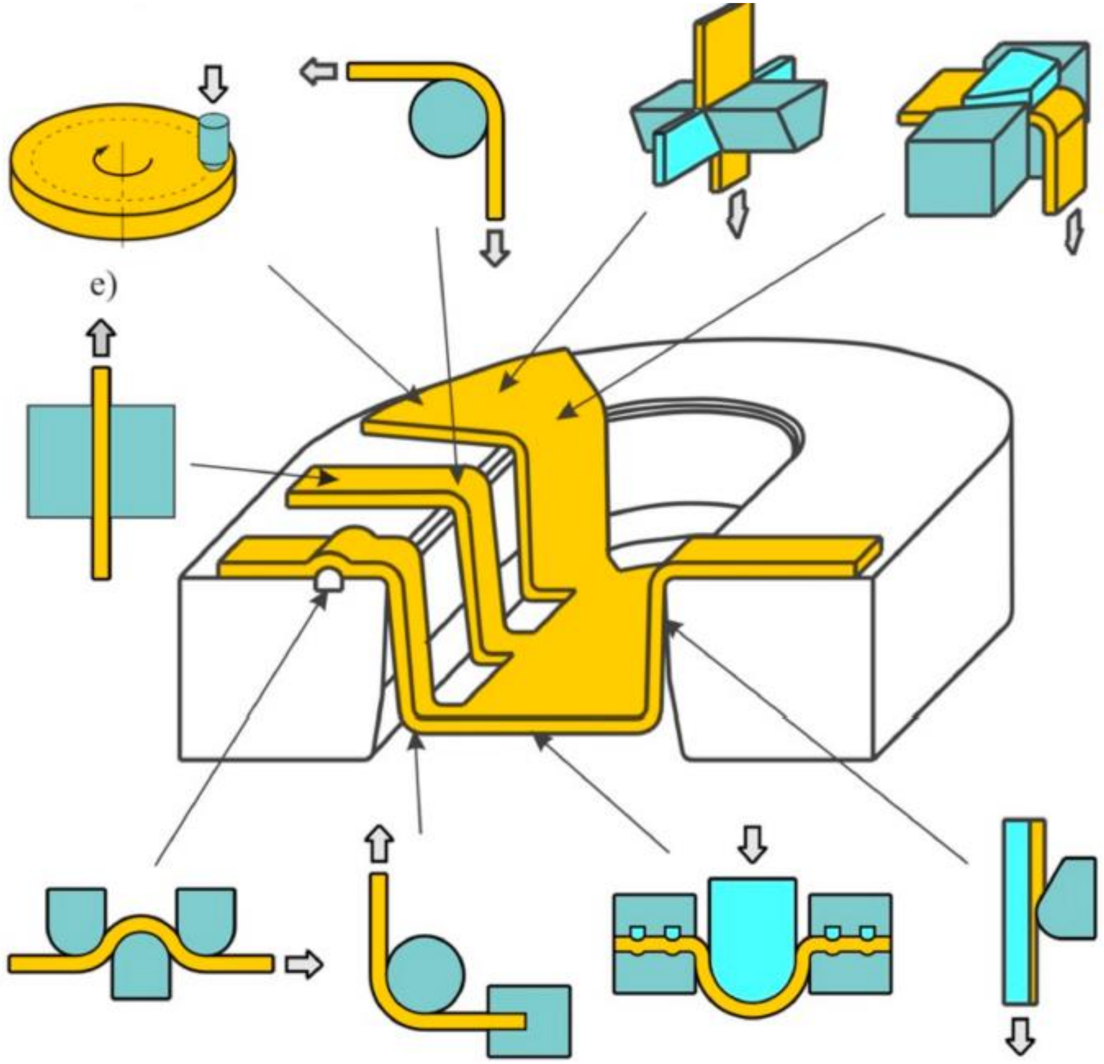

- Main **function of the draw-beads** is to increase the material flow resistance around the periphery of the part
  - ✓ Multiple bending-unbending
  - ✓ Reverse tension-compression loading over the sheet thickness

Main objective of the study

- Explore the potential of the **draw-bead test** to evaluate the **heat generated** by plastic deformation and friction

Adopted procedure

- Comparison between the **uniaxial tensile test** and the **draw-bead test** in terms of **temperature evolution**
- **Experimental analysis** of both tests, using an infrared thermal camera to measure the temperature
- **Thermo-mechanical finite element analysis** of both tests
- Dual phase steel **DP780** with an initial thickness of 0.8 mm

Experimental procedure

Uniaxial tensile test

- **Room temperature**
- Along the **rolling direction**
- Constant crosshead speed (1.3 mm/s)
- **Initial strain rate of 1.6×10^{-2} s^{-1}**

- One specimen surface was **coated with matt black paint**
  - ✓ Ensuring an emissivity close to 1
  - ✓ Improve the temperature field measurement with an infrared thermographic camera

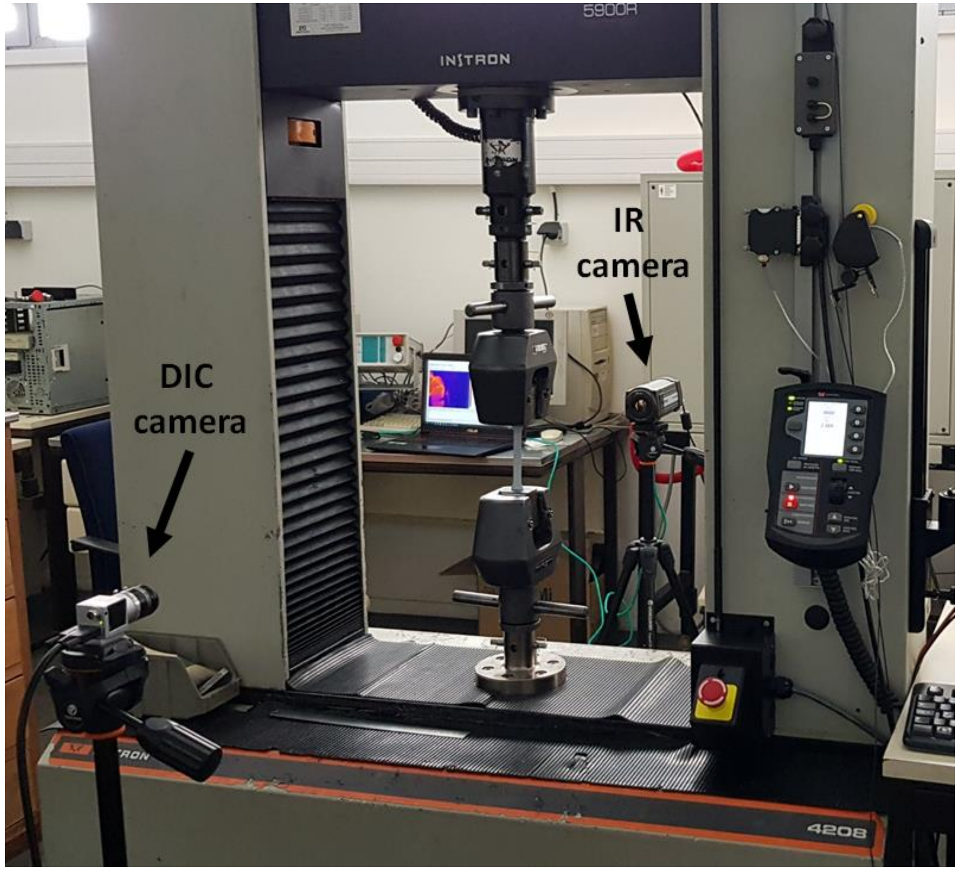

Experimental apparatus

Specimen surfaces

Experimental procedure

Draw-bead test

- All rollers have **21 mm of diameter**, while the dimensions of the **sheet strip are 450×25×0.8 mm**
- Full penetration (*p*=21.8 mm) and the side clearance between rollers was *c*=1.55 mm
- The process is divided in **3 phases**
  - ✓ The strip is bended by the vertical movement of the middle roller
  - ✓ The strip is pulled by a grip
  - ✓ The deformed strip springback

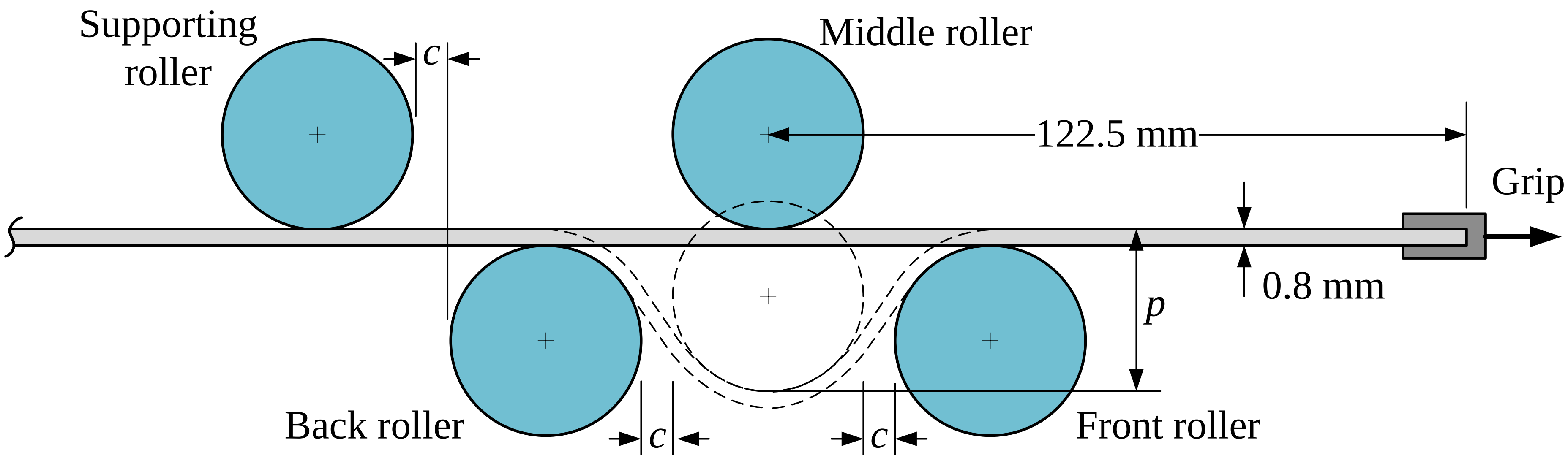

Experimental procedure

Draw-bead test

- The equipment used was designed to enable the tests to be **performed in a tensile test machine**
  - ✓ Allows changing the **penetration depth**, **side clearance** and the **pulling speed** of the grip
- The temperature field of the strip was measured with a **thermographic infrared camera** (FLIR A325), using an image resolution of 320×240 pixels matrix, at 60 frames/s

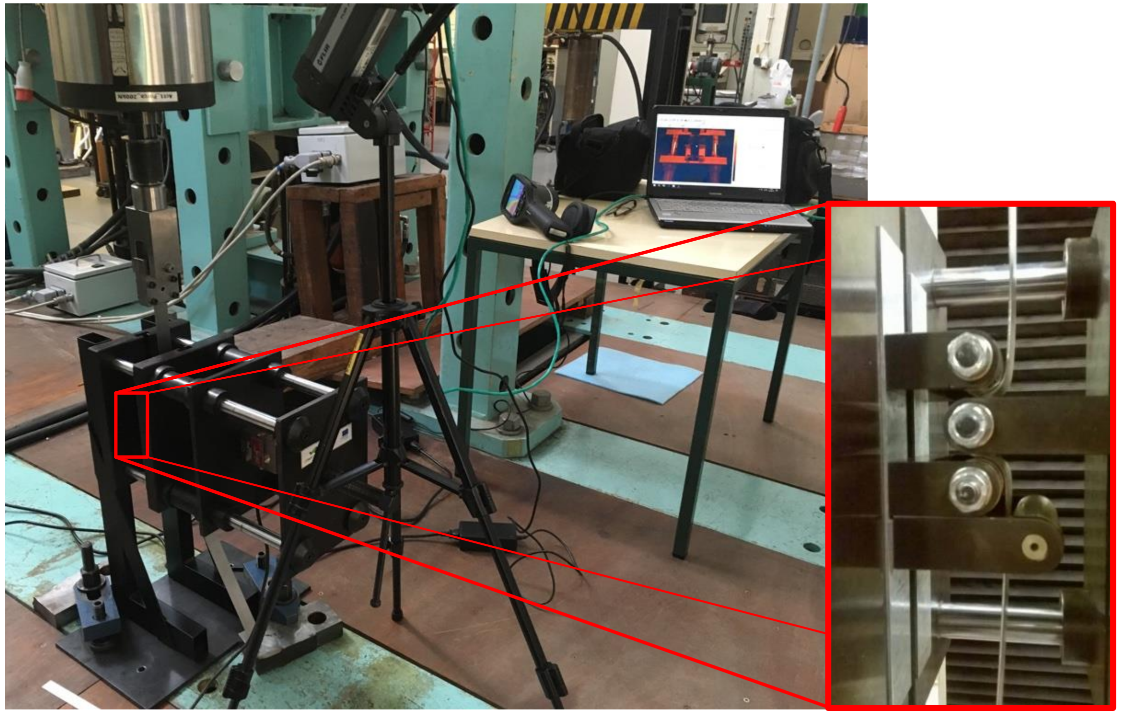

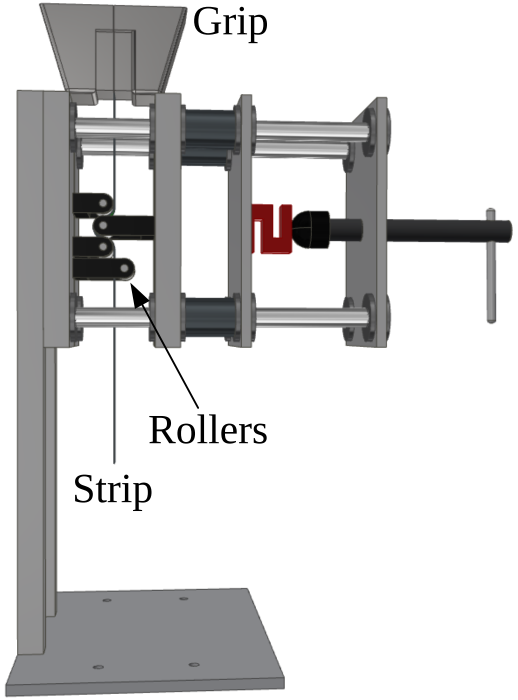

Transient thermo-mechanical analysis

- Numerical simulation of both the **uniaxial tensile test** and the **draw-bead tests** using the in-house implicit finite element code **DD3IMP**
  - ✓ Temperature independent elastoplastic behavior
  - ✓ Staggered algorithm for the thermo-mechanical coupling
  - ✓ Rollers are assumed rigid and isothermal
  - ✓ Specimens are discretized with 3D hexahedral finite elements (3 layer in thickness direction of the strip)
  - ✓ Strip discretized with 4167 elements (element size in the length direction is approximately 0.27 mm)
  - ✓ Friction behavior between the strip and the rollers defined by the Coulomb friction law

Thermal analysis

- Differential equation that defines the **thermal conduction within a solid**

$$\rho c_{\mathrm{p}} \frac{\partial T}{\partial t} - k\left(\frac{\partial^2 T}{\partial x^2} + \frac{\partial^2 T}{\partial y^2} + \frac{\partial^2 T}{\partial z^2}\right) - \dot{q}_{\mathrm{p}} - \dot{Q}_{\mathrm{f}} = 0$$

$\dot{q}_{\mathrm{p}}$: Thermal power generated by plastic deformation

$\dot{Q}_{\mathrm{f}}$: Thermal power generated by the friction forces

- **Thermal properties** of the dual phase steel DP780

Property	Value
Mass density	7900 kg/m^3
Specific heat capacity	450 J/(kg·K)
Thermal conductivity	40 W/(m·K)

Numerical model

Thermal analysis

- Thermal power generated by **plastic deformation**
  - ✓ Fraction of plastic power converted

$$\dot{q}_{\mathrm{p}} = \beta \dot{w}^{\mathrm{p}} = \beta(\boldsymbol{\sigma} : \dot{\boldsymbol{\varepsilon}}^{\mathrm{p}})$$

→ Constant Taylor–Quinney factor (0.9)

- Thermal power generated by the **friction forces**

$$\dot{Q}_{\mathrm{f}} = \eta(\mathbf{t}_{\mathrm{t}} \cdot \dot{\mathbf{g}}_{\mathrm{t}})$$

→ Heat equally portioned between the two contacting bodies (strip and rollers), thus η=0.5

Thermal analysis

- **Free convection** defined on the exterior surface

$$\dot{q}_{\text{conv}} = h_{\text{conv}}(T - T_{\infty})$$

→ Heat transfer coefficient in free convection

h_{conv}=5 W/m²·K

- **Contact conductance** defined on the exterior surface

$$\dot{q}_{\text{c}} = h_{\text{c}}(T - T_{\text{roller}}) = h_{\text{sup}} \exp(-m\, g_{\text{n}})(T - T_{\text{roller}})$$

→ Interfacial heat transfer coefficient

✓ Interfacial heat transfer coefficient depends on the gap distance between the strip and the roller

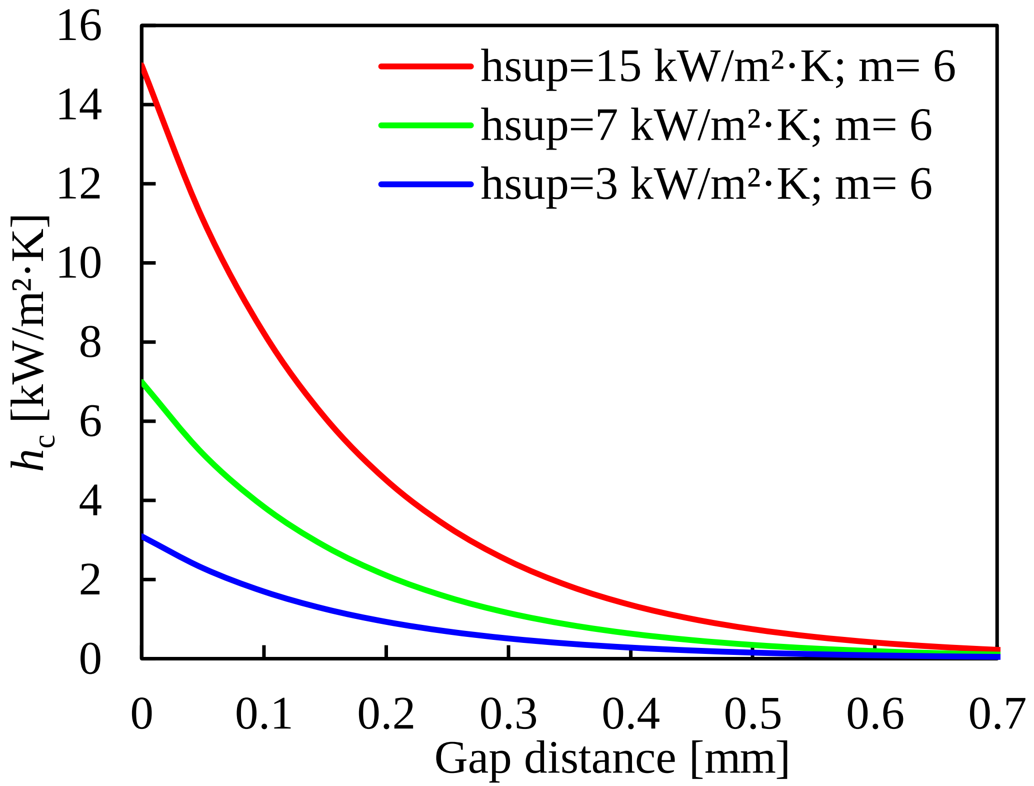

Mechanical analysis

- Mechanical behavior of **DP780** described by an **elastoplastic constitutive model**
  - ✓ Isotropic elastic behavior described by the Hooke's law (*E*=210 GPa and *ν*=0.30)
  - ✓ Plastic behavior described by an **isotropic work hardening law** (Swift) and a **yield criterion** (Hill'48)

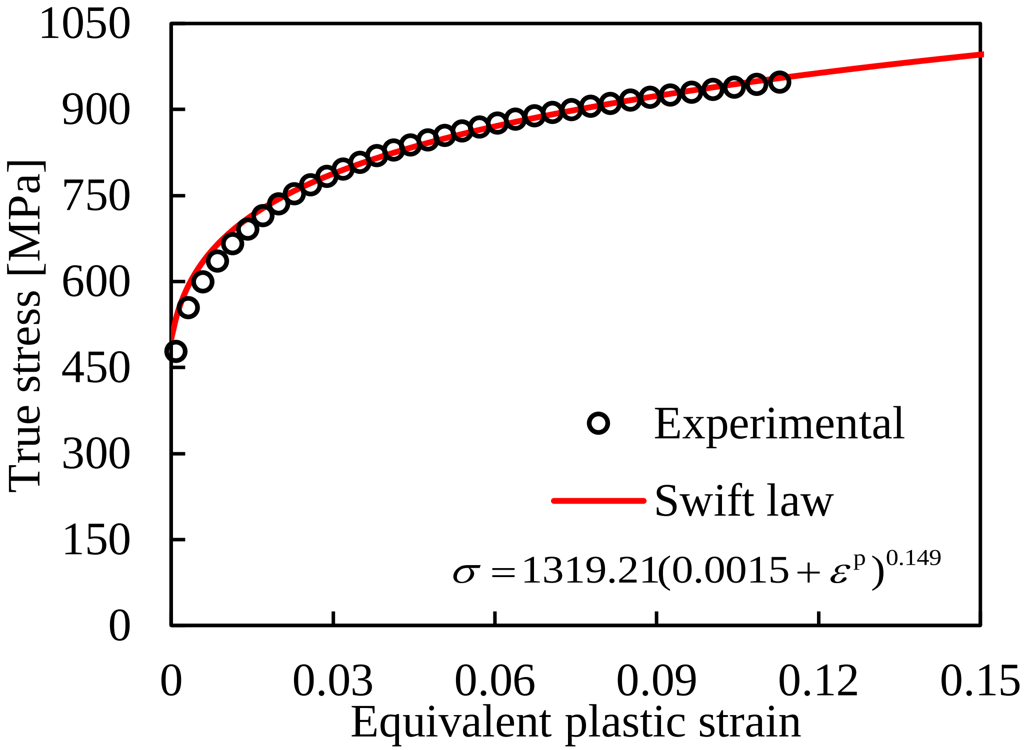

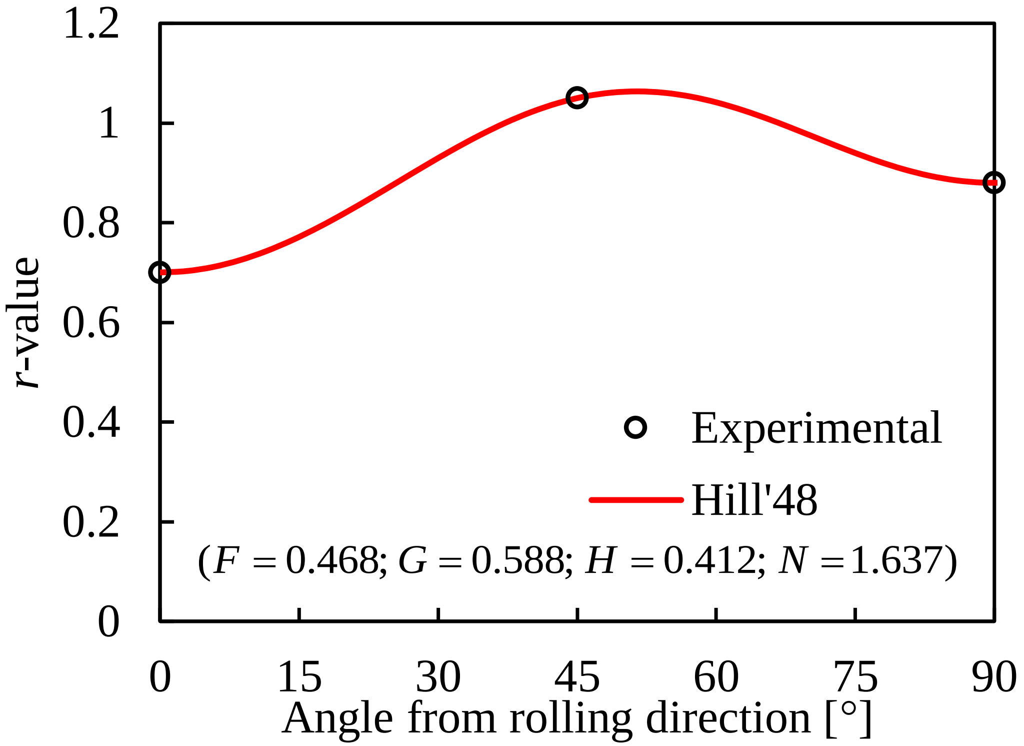

Uniaxial tensile test

- Comparison between **experimental** and **numerical** evolution of the temperature variation in the midpoint of the specimen
  - ✓ Numerical prediction is in **good agreement** with the experimental measurement
  - ✓ **Approximately linear rising** up to the onset of necking
  - ✓ Considering the instant of onset of necking, the predicted and experimental temperature rise is about 25ºC and 30ºC, respectively
  - ✓ The **onset of necking** is numerically predicted for a higher value of strain

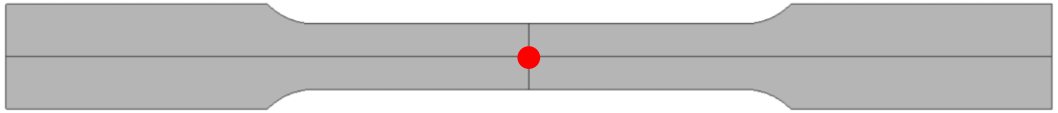

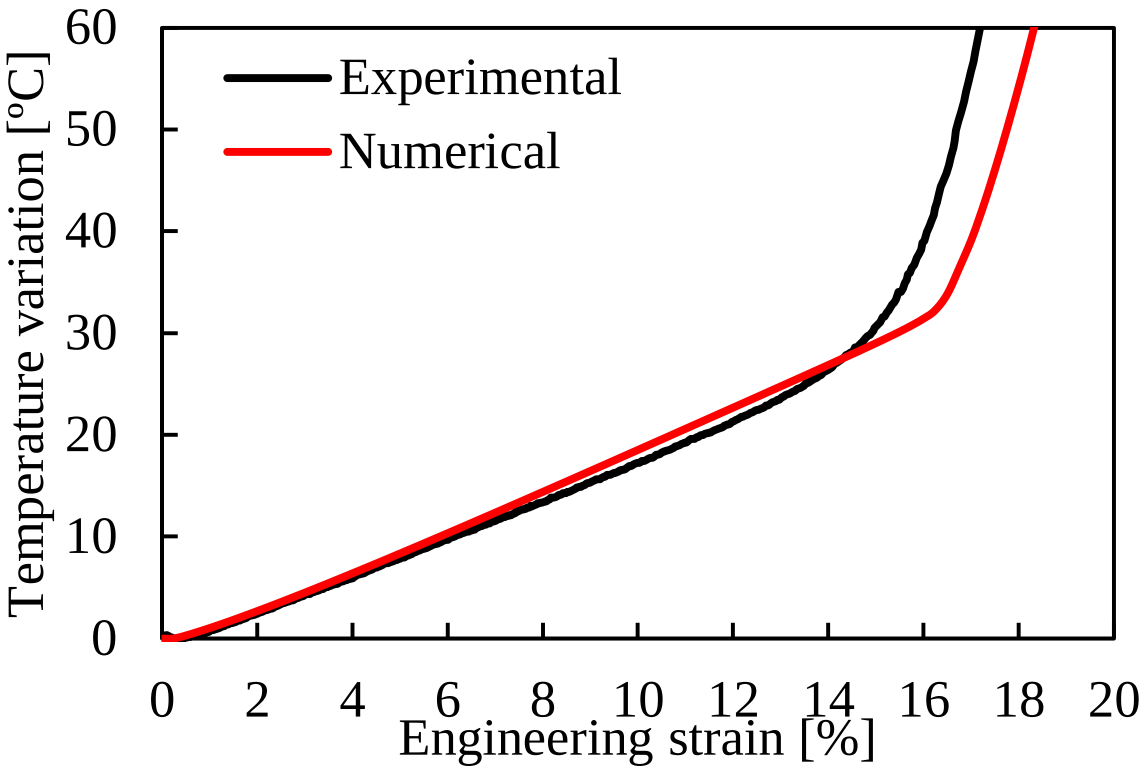

Uniaxial tensile test

- Distribution of the **predicted temperature** variation in the specimen for 3 different levels of engineering strain
  - ✓ The **maximum** temperature arises in the **center of the specimen**
  - ✓ The temperature rise in the specimen ends is negligible

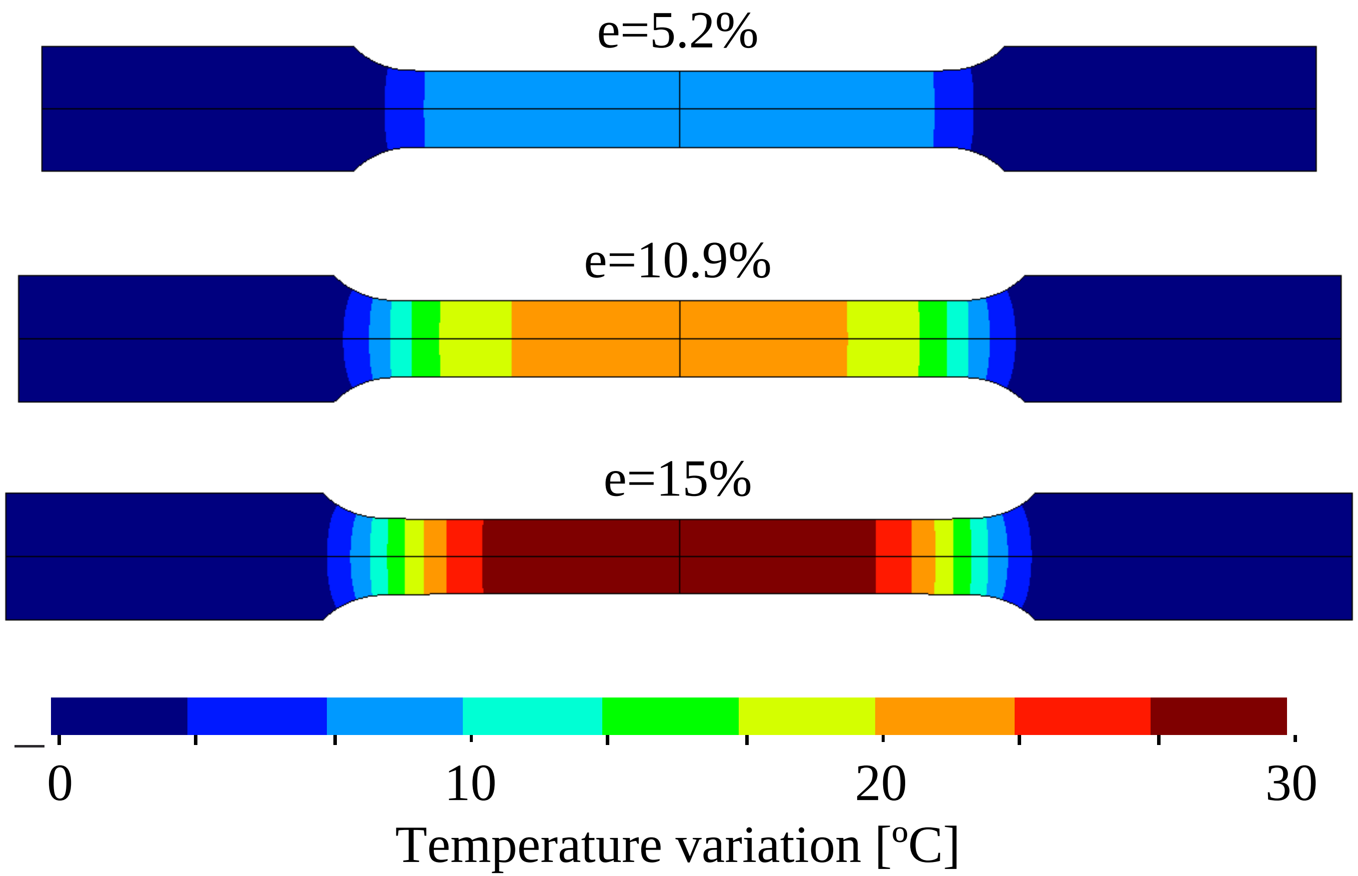

- Thus, the fraction of plastic power converted into heat (90%) and the heat transfer coefficient in free convection (5 W/m^2·K) were accurately selected

Uniaxial tensile test

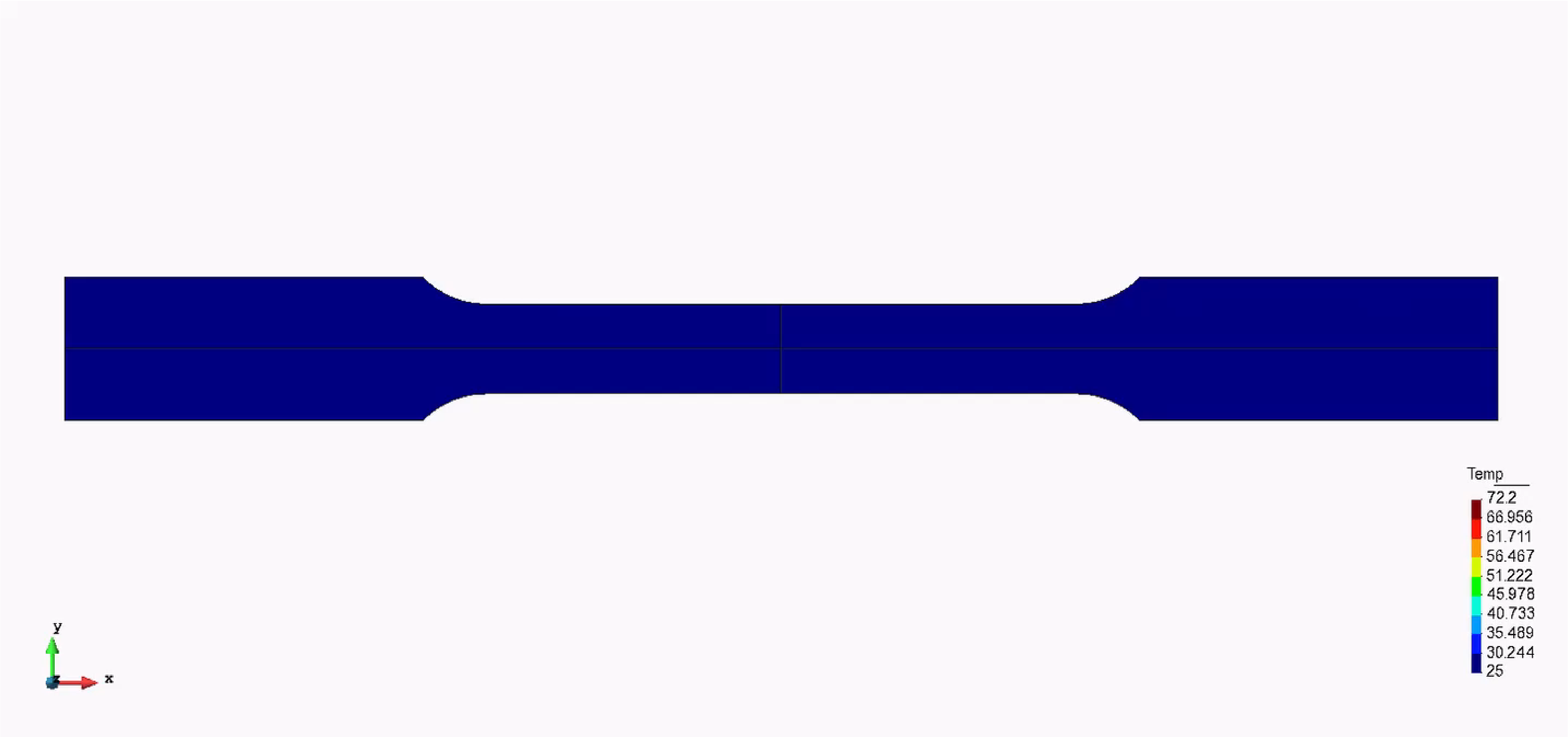

Draw-bead test

- **Experimental** evolution of the **pulling force** for different values of pulling speed
  - ✓ The **steady state** of the pulling force is quickly achieved after the initial sheet bending/unbending on the middle roller
  - ✓ There is no evidence that the pulling force is influenced by the pulling speed (results dispersion corresponds to the level of uncertainty in the measurements)
  - ✓ The force evolution is **approximately constant** during the pulling operation (about 2.5 kN)

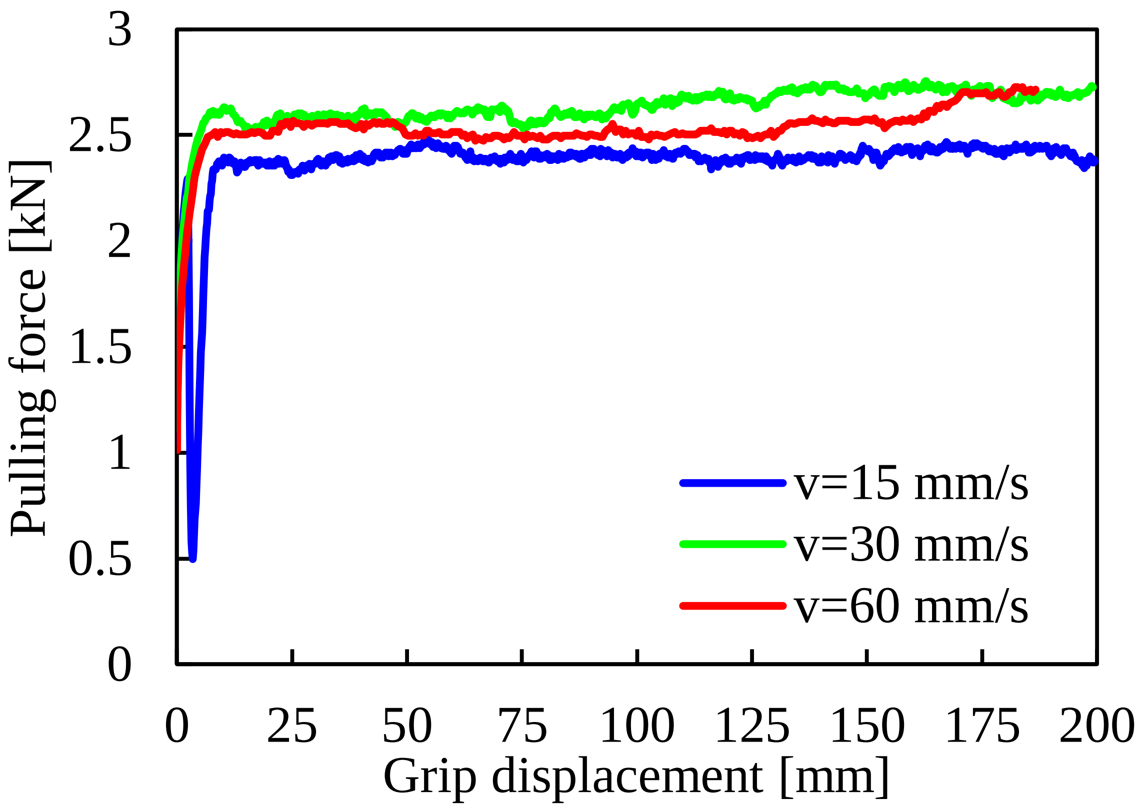

Draw-bead test

- **Numerical** evolution of the **pulling force** for different values of friction coefficient
  - ✓ The predicted pulling force is independent from the pulling speed since the constitutive model is not strain rate sensitive
  - ✓ The predicted pulling force is about 1.5 kN in the steady state regime considering the **frictionless condition** (μ=0.0)
  - ✓ The predicted pulling force is close to 2.5 kN for **μ=0.12**

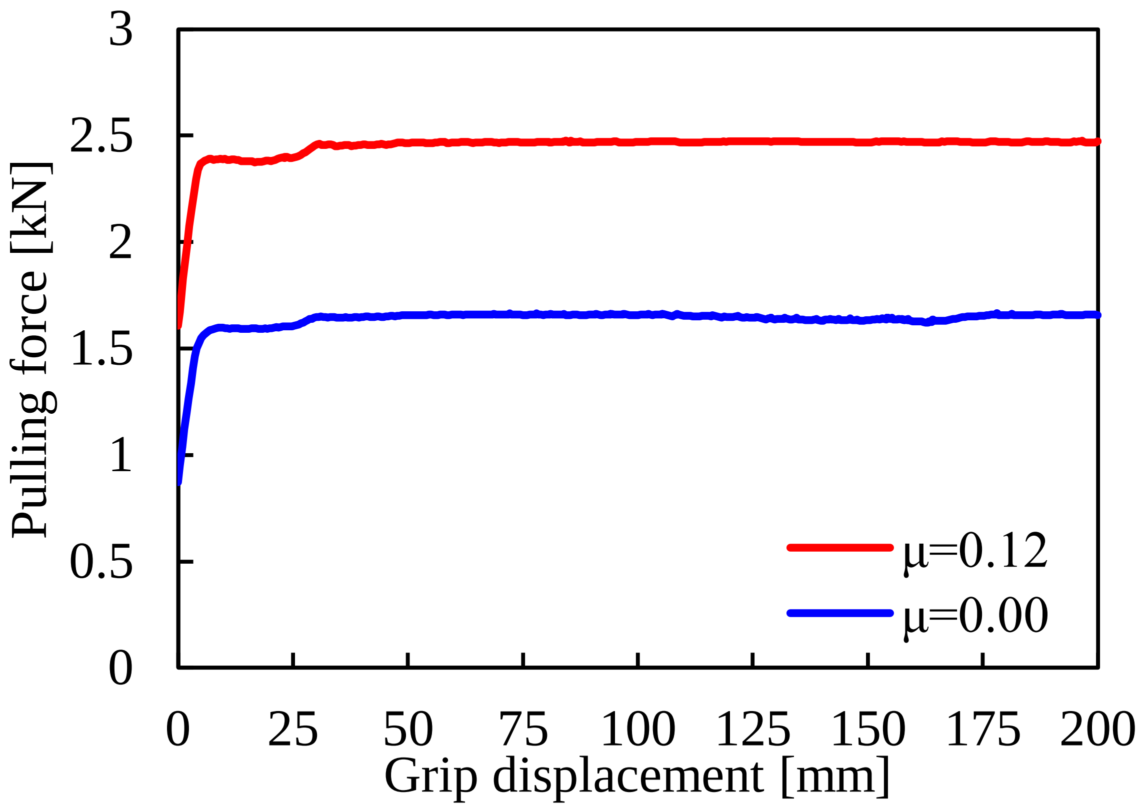

Draw-bead test

- **Experimental** profile of the strip after springback
  - ✓ The curved region of the strip sheet was subjected to **multiple bending-unbending** induced by the draw-bead geometry
  - ✓ A decrease of the pulling distance leads to a reduction of the springback angle

Draw-bead test

- Influence of the **friction coefficient** on the **predicted** profile of the strip after springback
  - ✓ The effect of the **friction coefficient** on the springback is **negligible**
  - ✓ The springback predicted numerically is significantly **lower** than the one measured experimentally
  - ✓ The inclusion of the kinematic hardening and the degradation of elastic stiffness due to plastic straining can improve the springback prediction

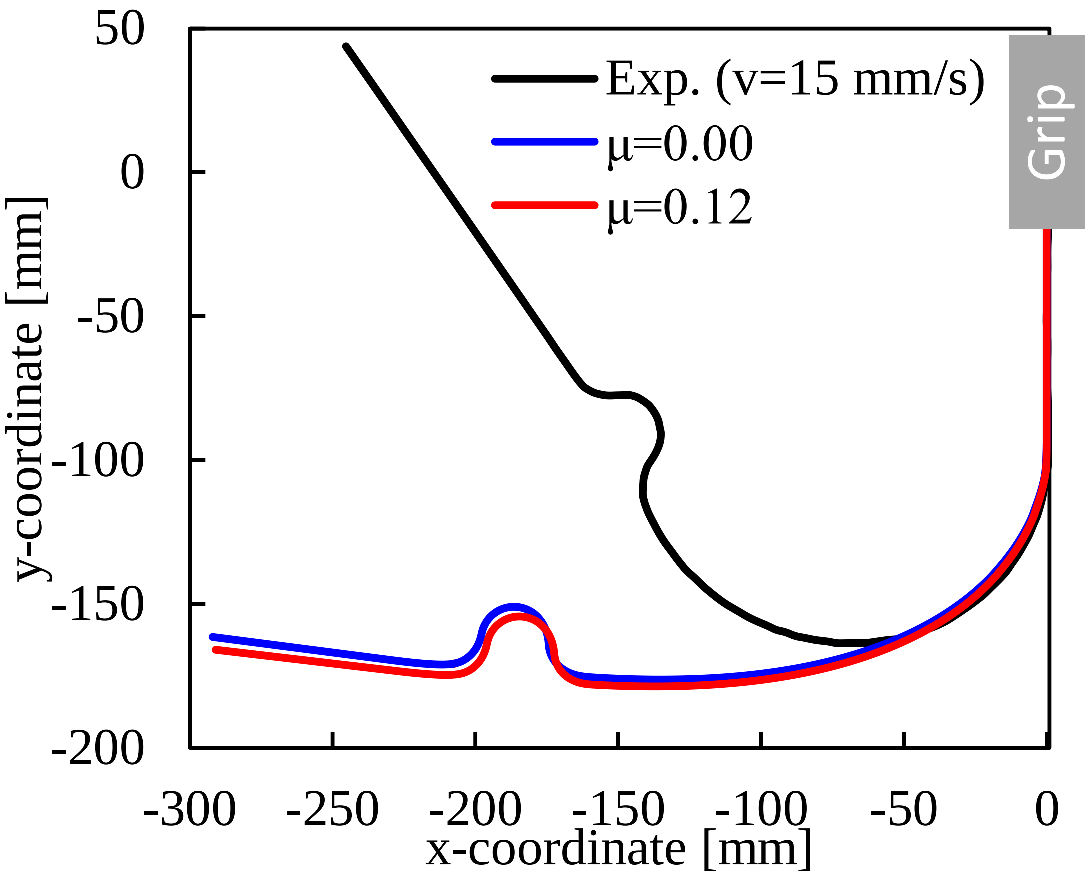

Draw-bead test

- **Predicted temperature variation** at 75 mm ahead the middle roller is presented for 3 different values of pulling speed
  - ✓ Increase the **pulling speed** leads to an **increase of the temperature** since the time available for the heat loss is lower
  - ✓ The increase of the **interfacial heat transfer coefficient** leads to a **decrease of the temperature** rise
  - ✓ The heat generated by plastic deformation and frictional contact occurs near the contact zones

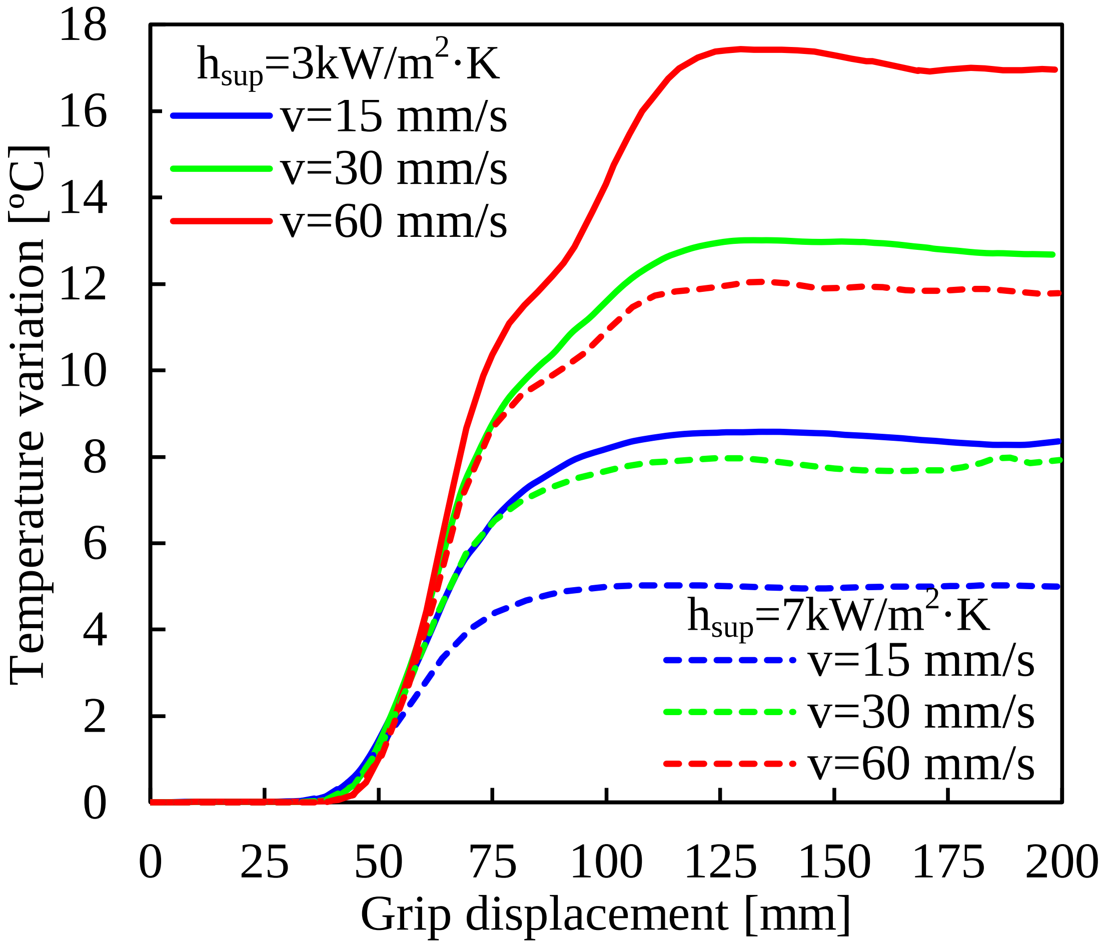

Draw-bead test

- Influence of the **grip velocity** on the temperature distribution measured by the IR camera

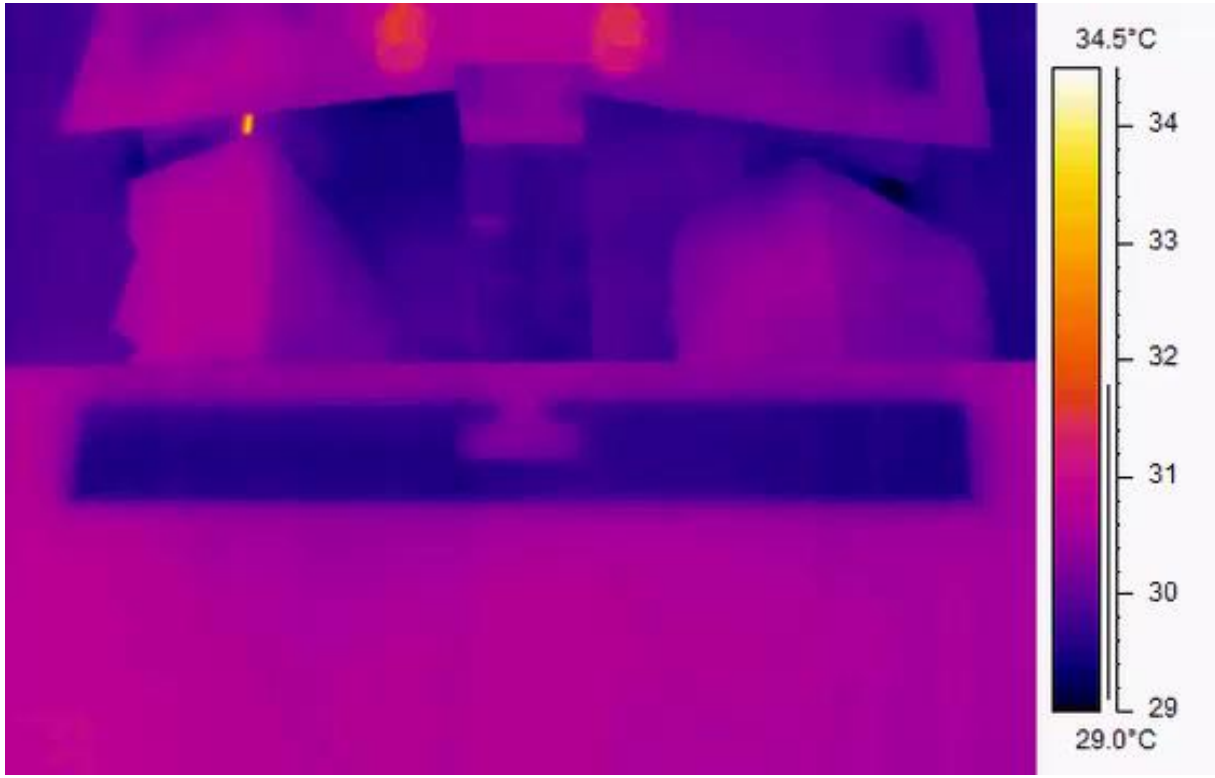

v=15 mm/s

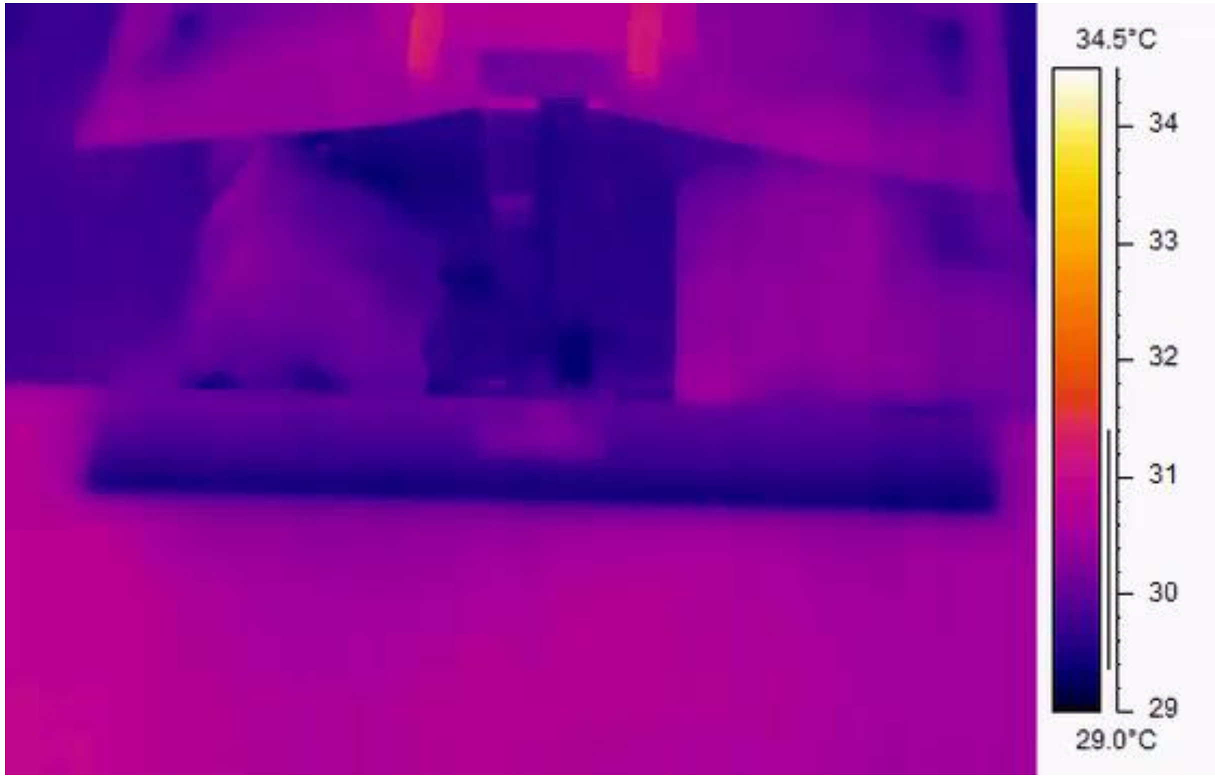

v=60 mm/s

Results and discussion

Draw-bead test

- Comparison between **experimental** and **numerical** temperature variation for h_{sup}=15 kW/m²·K
  - ✓ Despite the large value for the interfacial heat transfer coefficient, the temperature variation is overpredicted by the numerical model
  - ✓ Most of the **heat generated** comes from **plastic deformation**
  - ✓ The temperature rise is significantly larger in the uniaxial tensile test than in the draw-bead test due to the **heat lost by contact with the rollers**

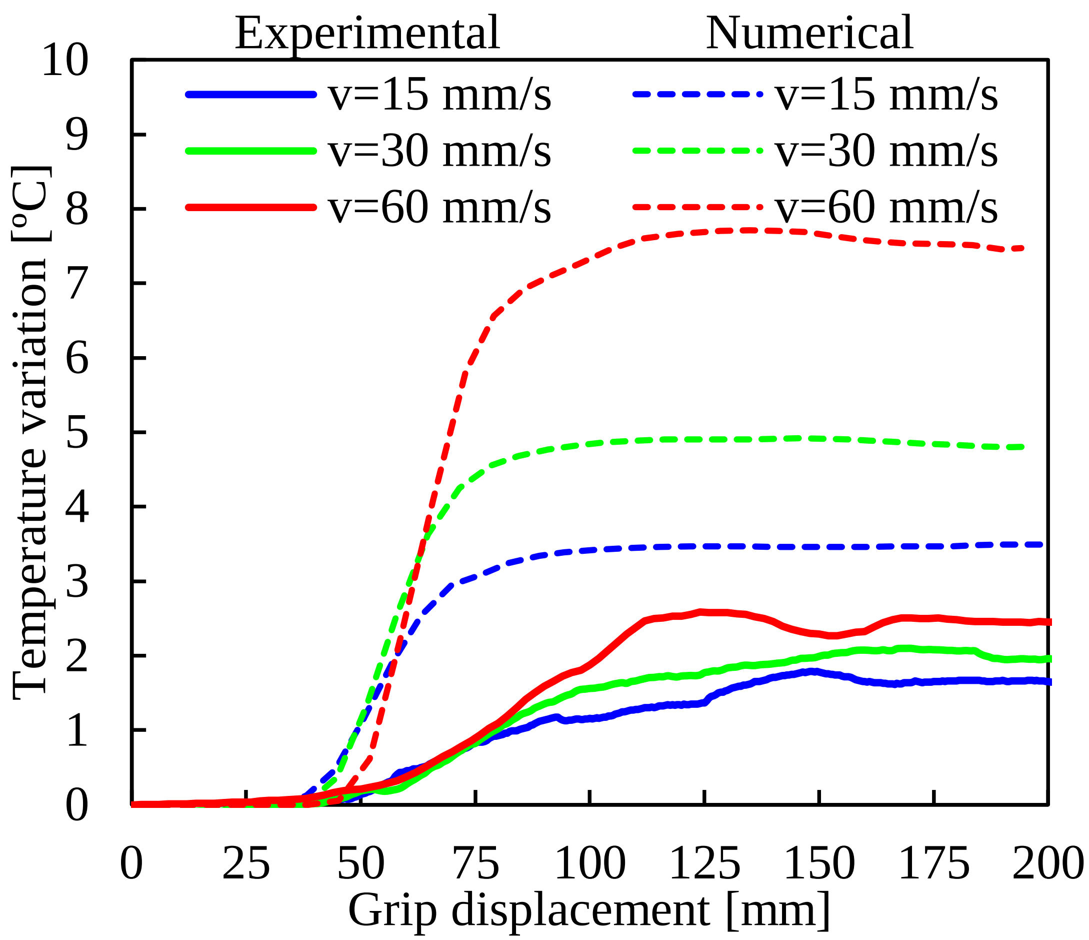

Conclusions

- **Experimental** and **numerical** thermo-mechanical analysis of **tensile and draw-bead tests**, using the **DP780 steel** with an initial thickness of 0.8 mm
- The **predicted temperature** rise in the **uniaxial tensile test** is in **good agreement** with the experimental measurement
- Comparing the numerical and experimental results from the **draw-bead test**, the pulling force is accurately predicted by the numerical model, but the springback is underestimated while the **temperature variation is overestimated**
- The predicted temperature variation is significantly affected by the adopted **interfacial heat transfer coefficient**
- The temperature rise is significantly **larger in the uniaxial tensile test than in the draw-bead test** due to the heat lost by contact with the rollers

Acknowledgements

The authors gratefully acknowledge Prof. Joaquim G. Mendes for the availability of IR thermal equipment used on this research. This work was funded by the Portuguese Foundation for Science and Technology (FCT) under projects with reference PTDC/EME-EME/30592/2017 and PTDC/EME-EME/31657/2017 and by European Regional Development Fund through the Portugal 2020 program and the Centro 2020 Regional Operational Programme (CENTRO-01-0145-FEDER-031657) under the project MATIS (CENTRO-01-0145-FEDER-000014) and UIDB/00285/202020.

Projetos Cofinanciados pela UE:

FCT Fundação para a Ciência e a Tecnologia

CENTRO 2020

PORTUGAL 2020

UNIÃO EUROPEIA
Fundo Europeu
de Desenvolvimento Regional

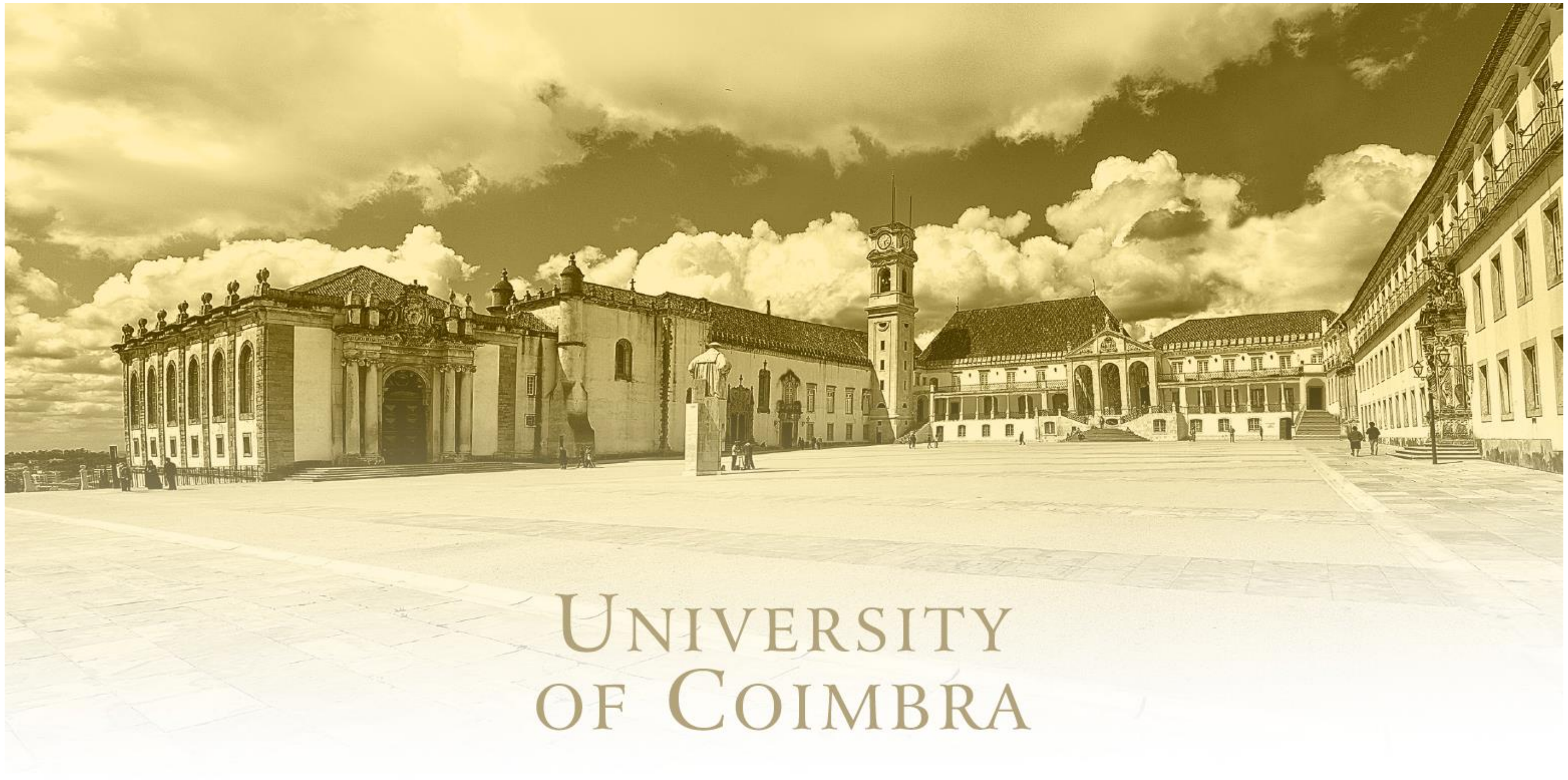

Thank you for watching!